ELSEVIER

Coordination Chemistry Reviews 237 (2003) 183–196

COORDINATION CHEMISTRY REVIEWS

www.elsevier.com/locate/ccr

Tetradentate Schiff base–oxovanadium(IV) complexes: structures and reactivities in the solid state

Masaaki Kojima [a,*], Hideki Taguchi [b], Masanobu Tsuchimoto [c], Kiyohiko Nakajima [d]

[a] *Department of Chemistry, Faculty of Science, Okayama University, Tsushima, Okayama 700-8530, Japan*
[b] *Research Laboratory for Surface Science, Faculty of Science, Okayama University, Tsushima, Okayama 700-8530, Japan*
[c] *Department of Chemistry, Faculty of Science and Technology, Keio University, Hiyoshi 3-14-1, Kohoku-ku, Yokohama 223-8522, Japan*
[d] *Department of Chemistry, Aichi University of Education, Igaya, Kariya 448-8542, Japan*

Received 25 January 2002; accepted 24 June 2002

Contents

Abstract

This article describes the crystal structures of several vanadium complexes containing tetradentate Schiff base ligands, and their properties and reactivities in the solid state. [VO{sal-(*R*,*R*)-stien}] (H_2sal-(*R*,*R*)-stien = *N*,*N*′-disalicylidene-(*R*,*R*)-1,2-diphenyl-1,2-ethanediamine) crystallized in two different forms, green (from dichloromethane and chloroform) and orange (from acetonitrile). X-ray structure analysis revealed that the green form contains mononuclear square-pyramidal molecules of the complex, whereas the orange form has a polynuclear linear chain structure. The green crystals turn orange when heated at 120 °C for a few minutes (thermochromism). Both forms are vapochromic, the orange crystals turning green on exposure to chloroform vapor, and the green crystals turning orange on exposure to acetonitrile vapor. The color of the orange complex changes to green on grinding (mechanochromism). [VO{3-EtOsal-(*R*,*R*)-2,4-ptn}] ($H_2$3-EtOsal-(*R*,*R*)-2,4-ptn = *N*,*N*′-di-3-ethoxysalicylidene-(*R*,*R*)-2,4-pentanediamine) also crystallizes in two different forms, green and orange. The polymeric orange crystals turn into the monomeric green form upon heating at 170 °C for 10 min. The mechanism of this conversion was studied using X-ray structure analysis and thermal analysis. Thermal isomerization in the solid state between a pair of diastereomers, **I** and **II**, of the oxovanadium(IV) complex with an unsymmetrical tetradentate Schiff base ligand, [VO{3-EtOsal,sal-(*R*,*R*)-chxn}] ($H_2$3-EtOsal,sal-(*R*,*R*)-chxn = *N*-salicylidene-*N*′-3-ethoxysalicylidene-(*R*,*R*)-1,2-cyclohexanediamine), was studied at 195 °C. The two diastereomers were separated using column chromatography, and each crystallized in two different colors: green (monomeric) and orange (polymeric). The orange complexes, **I** (orange) and **II** (orange), turned green on heating at 195 °C for a few minutes. All four complexes, **I** (green), **II** (green), **I** (orange), and **II** (orange), undergo isomerization at 195 °C to yield an equilibrium mixture, **I**:**II** ≈ 1:1. On heating [VO(3-EtOsal-*meso*-stien)] ($H_2$3-EtOsal-*meso*-stien = *N*,*N*′-di-3-ethoxysalicylidene-(*R*,*S*)(*S*,*R*)-1,2-diphenyl-1,2-ethanediamine) at 190 °C for 8 h, dehydrogenation took place at the two benzylic carbon atom sites to form a C = C double bond

* Corresponding author. Tel./fax: +81-86-251-7842
E-mail address: kojima@cc.okayama-u-ac.jp (M. Kojima).

PII: S0010-8545(02)00227-8

in the five-membered N–N chelate ring moiety. A vanadium(V) species formed on heating the starting complex in the air will be the oxidant of the thermal dehydrogenation reaction.

Keywords: Vanadium complex; Schiff base complex; Thermochromism; Vapochromism; Mechanochromism; Thermal dehydrogenation

1. Introduction

In 1986, we reported on the asymmetric oxidation of sulfides into the corresponding sulfoxides using organic hydroperoxides catalyzed by optically active Schiff base–oxovanadium(IV) complexes [1,2]. The complexes used for the asymmetric catalytic reactions involved tetradentate Schiff base ligands derived from optically-active 1,2-diamines and salicylaldehyde (or its derivatives). Such complexes are usually green and in the solid state have a monomeric five-coordinate square pyramidal structure. However, a few orange oxovanadium(IV) complexes have also been reported [3–5]. In these species, a vanadyl oxygen atom of one molecule coordinates to the sixth position of a vanadium atom in a neighboring molecule, resulting in an infinite chain structure. Both monomeric green and polymeric orange crystals of {*N*,*N*′-disalicylidene-(*R*,*R*)-1,2-diphenyl-1,2-ethanediamine}oxovanadium(IV), [VO{sal-(*R*,*R*)-stien}] (Fig. 1) were obtained on crystallization of the complex from different solvents [6,7]. During IR measurements on the orange species in a KBr pellet, we encountered a phenomenon called mechanochromism; the color of the complex changed from orange to green upon grinding in a mortar. The crystals of the complex also showed a reversible color change between orange and green when exposed to vapors of organic solvents (vapochromism). The green crystals turned orange when heated (thermochromism). We were fascinated with these color changes, and studied the mechanism of the interconversion using their crystal structures.

A closely related complex, [VO(3-EtOsal-*meso*-stien)] (Fig. 1, $H_2$3-EtOsal-*meso*-stien = *N*,*N*′-di-3-ethoxysalicylidene-(*R*,*S*)(*S*,*R*)-1,2-diphenyl-1,2-ethanediamine) underwent thermal dehydrogenation to form [VO(3-EtOsalton)] ($H_2$3-EtOsalton = *N*,*N*′-di-3-ethoxysalicylidene-1,2-diphenyl-1,2-ethenediamine), which has a C=C double bond in the five-membered chelate ring moiety [8]. We have also studied the thermal isomerization between a pair of diastereomers of a vanadium complex with an unsymmetrical tetradentate Schiff base ligand [9].

In this paper, we report on the crystal structures of several vanadium complexes containing tetradentate Schiff base ligands, along with their properties and reactivities in the solid state.

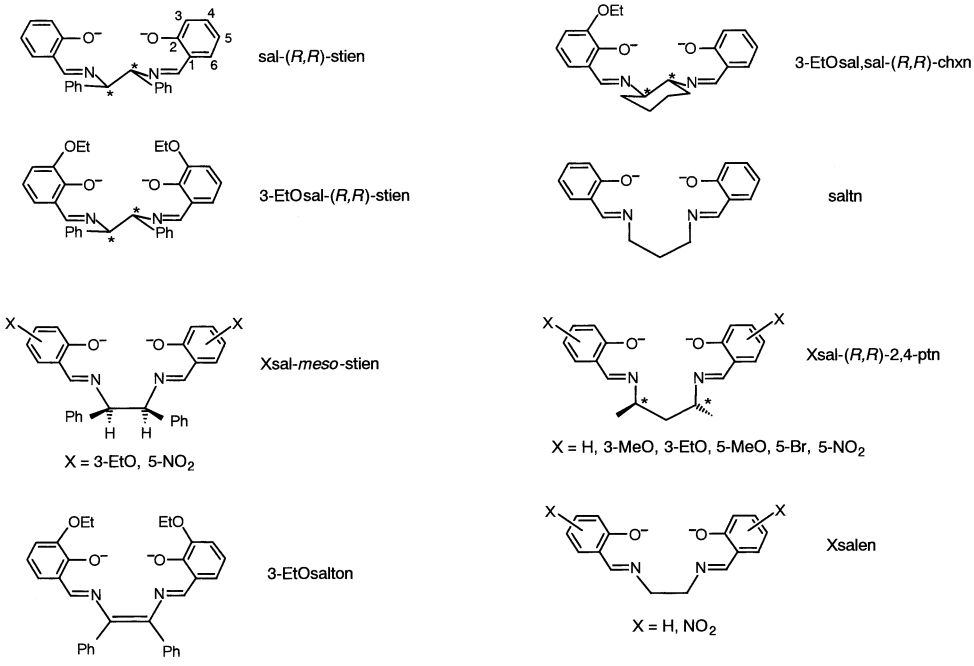

Fig. 1. The tetradentate Schiff base ligands studied in this paper.

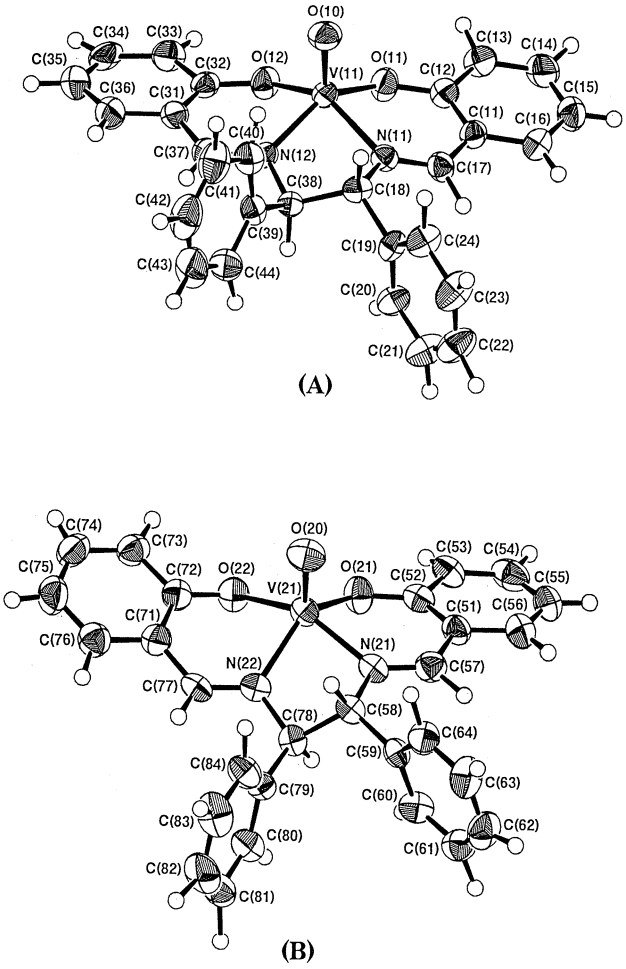

Fig. 2. An ORTEP drawing of [VO{sal-(*R*,*R*)-stien}] · CH_3OH (**1**), with the methanol molecule omitted. Reproduced with permission from Ref. [6].

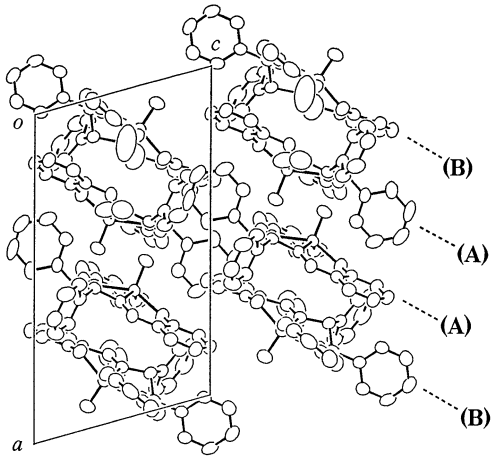

Fig. 3. Projection of the crystal structure of [VO{sal-(*R*,*R*)-stien}] · CH_3OH (**1**) viewed along the *b*-axis. Reproduced with permission from Ref. [6].

2. Monomeric and polymeric forms of Schiff base–oxovanadium(IV) complexes

2.1. Structures and mechano-, thermo-, and vapochromism of [VO{sal-(R,R)-stien}]

The reaction of $[VO(acac)_2]$ (acac = 2,4-pentanedionate ion) with the H_2sal-(*R*,*R*)-stien ligand in dichloromethane yielded green crystals of [VO{sal-(*R*,*R*)-stien}]. These green crystals were recrystallized from chloroform. In contrast, the recrystallization of the green complex from acetonitrile produced orange crystals. When the orange complex was dissolved in chloroform or dichloromethane, the color of the solution was green and the absorption spectrum was identical to that of the green complex. Pasini and Gullotti have discussed the spectroscopic data of several green and orange Schiff base–oxovanadium(IV) complexes [10]. However, there has been no report on the crystal structures of both orange and green forms of a single complex. Figs. 2 and 3 show, respectively, the molecular and crystal structures of the green complex [VO{sal-(*R*,*R*)-stien}] · CH_3OH (**1**). The two independent molecules in the unit cell, A and B, face each other, disposing the V=O groups in the opposite directions. A and B differ slightly from one another with respect to the orientation of the phenyl rings of the Schiff base ligand. The geometry around each vanadium atom is a distorted square pyramid with the oxo ligand in the apical position. The distance between V(11) (A) and V(21) (B) is 6.297(3) Å and no interaction between the two vanadium atoms is suggested.

The orange form, [VO{sal-(*R*,*R*)-stien}] · CH_3CN (**2**), consists of individual complexes stacked to give an infinite linear ···V=O···V=O··· chain. Fig. 4 shows a portion of the infinite chain, and Fig. 5 shows the packing diagram in the unit cell. The two metal complex subunits in the unit cell, C and D, differ by a 180° rotation but otherwise have identical structural parameters. The oxo bridging groups are distinctly nonsymmetric. The V=O bond distances [V(1A)–O(1A); 1.625(5) Å and V(1B)–O(1B); 1.636(5) Å] are longer than those of **1** [1.604(4) and 1.595(4) Å]. The latter bond lengths are within the range of a typical V=O distance (1.57–1.62 Å). The bond distances of V(1A)–O(1B) and V(1B)–O(1A), 2.188(5) and 2.196(5) Å, respectively, are slightly shorter than the corresponding bond distance (2.213(9) Å) of the polymeric [VO(saltn)] (Hsaltn = *N*,*N*′-disalicylidene-1,3-propanediamine) complex [3]. Solvents of crystallization ($CHC1_3$ in **1** and CH_3CN in **2**) are not associated with any metal atom.

Fig. 6 shows the reflection spectra of the complexes. A broad band at 590 nm of the green complex **1** corresponds to the d–d absorption band in dichloromethane (592 nm). Complex **2** showed an absorption band around 920 nm. The IR spectra of **1** and **2** in Nujol

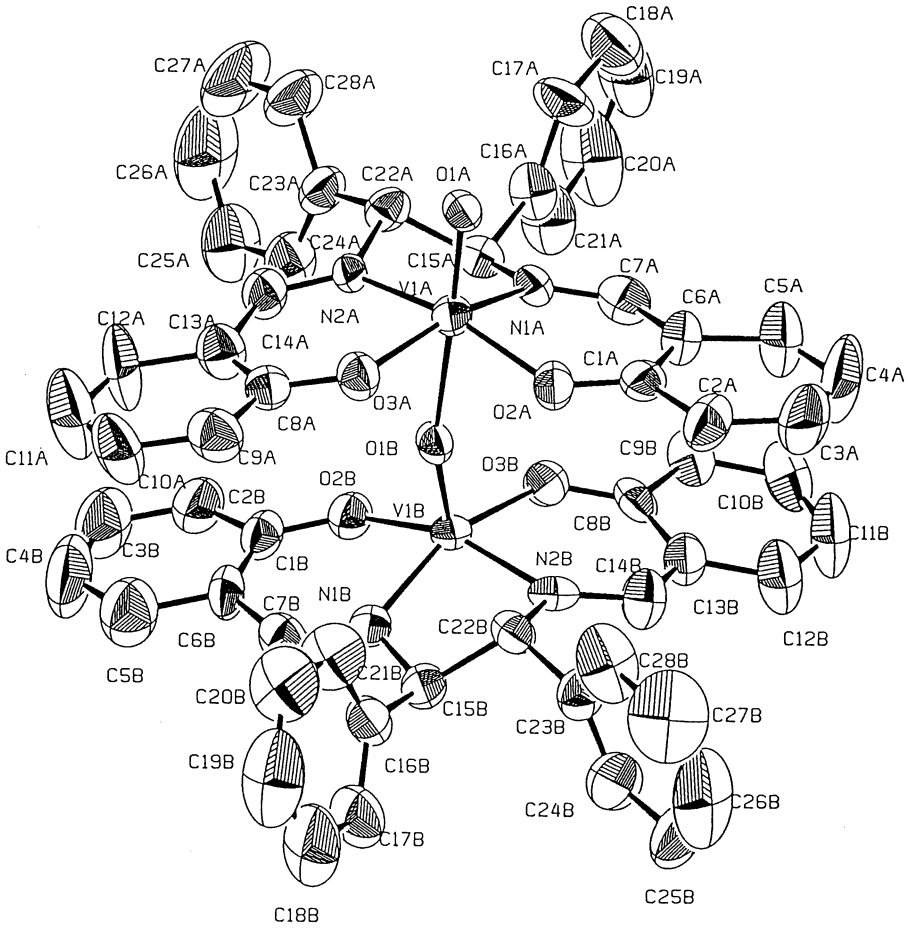

Fig. 4. An ORTEP drawing of [VO{sal-(*R*,*R*)-stien}] · CH_3CN (**2**), with the acetonitrile molecule omitted. Reproduced with permission from Ref. [6].

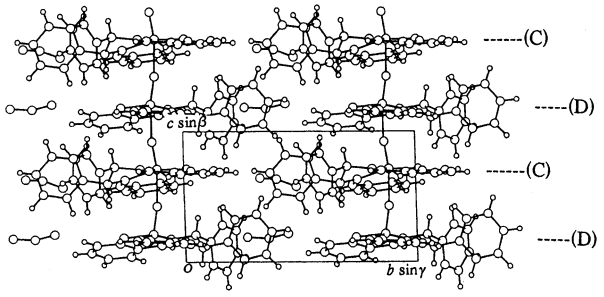

Fig. 5. Projection of the crystal structure of [VO{sal-(*R*,*R*)-stien}] · CH_3CN (**2**) viewed along the *a*-axis. Reproduced with permission from Ref. [6].

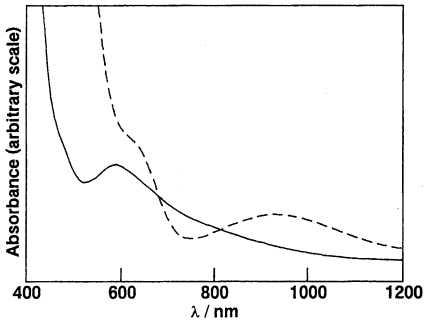

Fig. 6. Reflection spectra of [VO{sal-(*R*,*R*)-stien}] · CH_3OH (**1**) (—) and [VO{sal-(*R*,*R*)-stien}] · CH_3CN (**2**) (– – –). Reproduced with permission from Ref. [7].

mulls showed the V=O stretching at 990 and 860 cm^{-1}, respectively. Coordination of the oxo-oxygen atom to an adjacent vanadium atom lengthens and weakens the V=O bond, lowering the V=O stretching frequency in the orange complex. Complex **2** shows mechanochromism (Fig. 7); the color of the crystals changes from orange to green on grinding and the green product obtained showed the V=O stretching band at 990 cm^{-1} in addition to the original 860 cm^{-1} absorption band. The intensity ratio between the two bands (990 and 860 cm^{-1}) indicates the proportion of disassembling, and depends on the extent of grinding. We measured the IR spectrum of a sample obtained by thoroughly grinding **2** with a mortar and pestle, and found that about 90% of **2** had been converted to the green form. A similar conclusion was deduced using EXAFS. We studied the stability of the orange and green crystals with pressure and heat. Both complexes **1** and **2** were very resistant to pressure; the complexes were pressed at 10^9 Pa for a few

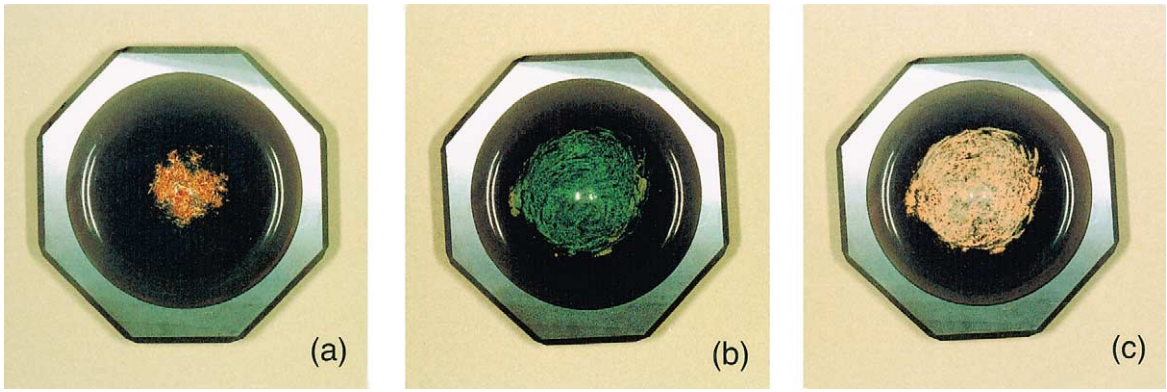

Fig. 7. A series of photographs showing the color change of [VO{sal-(*R*,*R*)-stien}]: (a) orange crystals of [VO{sal-(*R*,*R*)-stien}] · CH_3CN (**2**); (b) the green product obtained by grinding **2** in a mortar; and (c) the regenerated orange form obtained by moistening the green product with a small volume of acetonitrile.

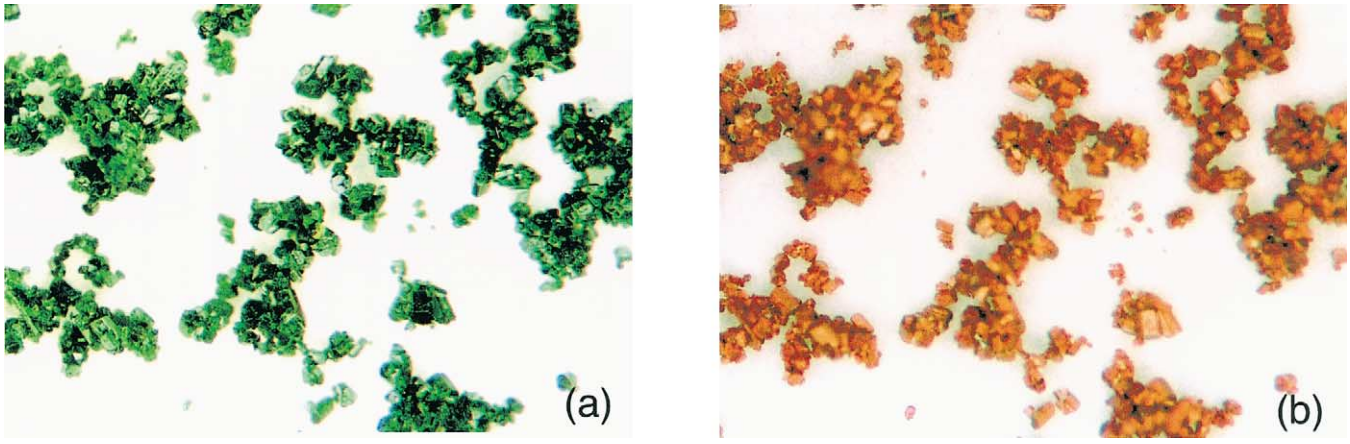

Fig. 8. (a) Green crystals of [VO{sal-(*R*,*R*)-stien}] · CH_3OH (**1**) and (b) orange crystals generated by exposing [VO{sal-(*R*,*R*)-stien}] · CH_3OH (**1**) to acetonitrile vapor.

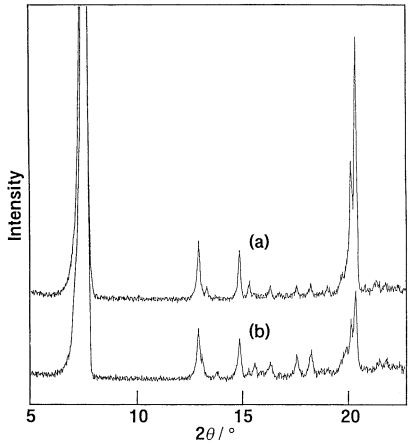

Fig. 9. X-ray powder diffraction patterns of the orange samples: (a) [VO{sal-(*R*,*R*)-stien}] · CH_3CN (**2**); and (b) orange crystals generated by exposing [VO{sal-(*R*,*R*)-stien}] · CH_3OH (**1**) to acetonitrile vapor. Reproduced with permission from Ref. [7].

minutes, but their color did not change. The color of **2** (the orange form) remained unchanged even after heating at 150 °C for 2 h. On the other hand, **1** (the green form) showed thermochromism; it turned orange when heated at 120 °C for a few minutes. Both forms remained unchanged when they were cooled to a very low temperature (−196 °C). Grinding presumably cleaves the ···V=O···V=O··· bonds to yield mononuclear species. The color of the green product obtained by grinding reverted to orange when moistened with a small volume of acetonitrile (Fig. 7c). The color change from green to orange suggests a reformation of the polymeric linear-chain structure. This color change could be made repeatedly.

We also observed vapochromism. The orange crystals **2** turned green upon exposure to chloroform vapor, and the green crystals **1** turned orange when exposed to acetonitrile vapor (Fig. 8). Accordingly, X-ray powder diffraction measurements on these samples were carried out. Fig. 9 compares the X-ray powder diffraction patterns of the orange samples. The diffraction pattern of **2** (Fig. 9a) and that of the orange crystals obtained by exposing the green crystals to acetonitrile vapor (Fig. 9b) are almost identical, and we concluded that the structure of these two samples was the same. Since two

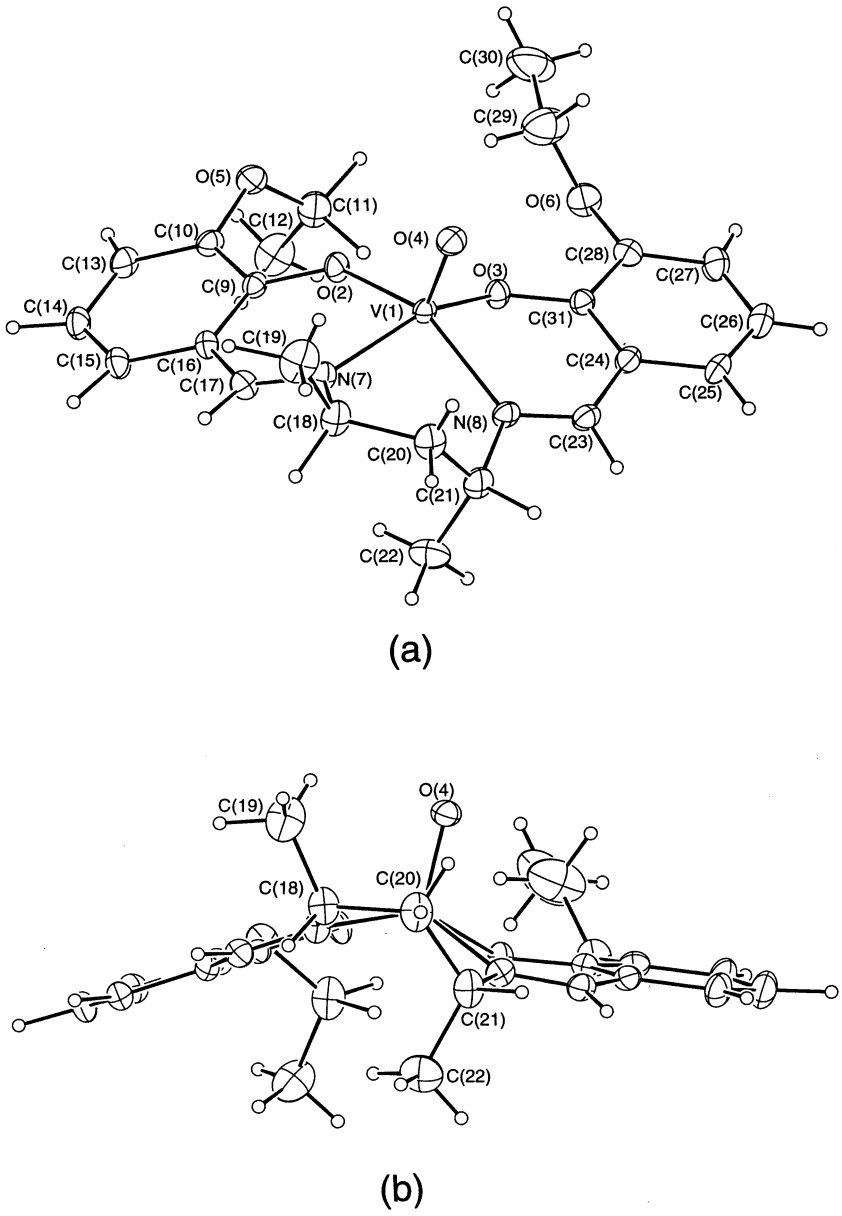

Fig. 10. A perspective view (a), and a side view (b) of the green [VO{3-EtOsal-(*R*,*R*)-2,4-ptn}] (**3**) complex. Reproduced with permission from Ref. [14].

independent molecules, A and B, face each other in the crystal of **1** (Fig. 3), a substantial rearrangement of the molecular orientation is required for it to transform into **2**. The green product obtained by grinding **2** ([VO{sal-(*R*,*R*)-stien}] · CH_3CN) was not crystalline. Probably, the loss of crystallinity is related to the evaporation of the acetonitrile molecule. Recently, Cariati et al. reported solvent- and vapor-induced isomerization between polymeric [CuI(4-pic)] (4-pic = 4-picoline) and tetramer $[CuI(4\text{-pic})]_4$ [11,12]. Exposure of the polymer to vapor or liquid toluene led to the formation of the tetramer, and the process could be reversed when the latter was exposed to pentane in the liquid or vapor form.

2.2. Interconversion between the monomeric and polymeric forms of [VO{3-EtOsal-(R,R)-2,4-ptn}]

Oxovanadium(IV) complexes containing tetradentate Schiff base ligands derived from 1,3-diamines such as 1,3-propanediamine and salicylaldehyde (or its derivatives) are usually orange, and the coordination geometry around vanadium is distorted octahedral. For example, in [VO(saltn)] [3] (Fig. 1) and [VO(saltn)(DMSO)] [13] (DMSO = dimethyl sulfoxide), a terminal oxygen atom (V=O) of the adjacent molecule and a solvent molecule, respectively, occupy the sixth position *trans* to the oxo atom. Upon introduction of bulky substituents into the six-membered N–N chelate ring moiety, one may obtain

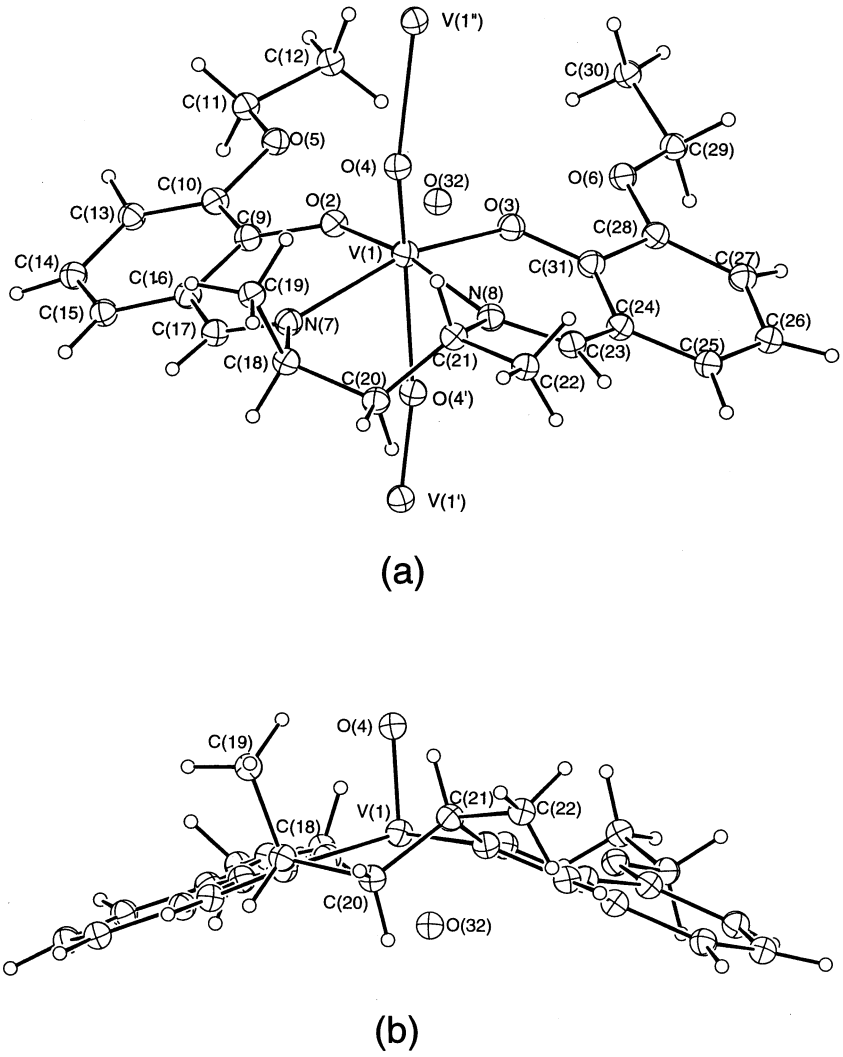

Fig. 11. A perspective view (a), and a side view (b) of the orange [VO{3-EtOsal-(*R*,*R*)-2,4-ptn}] · H_2O (**4**) complex. Reproduced with permission from Ref. [14].

both monomeric five-coordinate square-pyramidal and polynuclear linear-chain forms according to the magnitude of the inter- and intramolecular steric repulsions caused by the substituents. We obtained both forms of [VO{3-EtOsal-(*R*,*R*)-2,4-ptn}] (Fig. 1, $H_2$3-EtOsal-(*R*,*R*)-2,4-ptn = *N*,*N*′-di-3-ethoxysalicylidene-(*R*,*R*)-2,4-pentanediamine), and studied the mechanism of the interconversion between the two forms from their crystal structures and by thermal analysis [14].

Reaction of vanadyl sulfate with the Schiff base ligand in methanol gave a green powder of [VO{3-EtOsal-(*R*,*R*)-2,4-ptn}] (**3**). The orange form, [VO{3-EtOsal-(*R*,*R*)-2,4-ptn}] · H_2O (**4**), was prepared by suspending **3** in a water–acetonitrile mixture (4: 1 (v/v)) and allowing this to stand for 4 days at room temperature, with occasional stirring. The IR spectra of **3** and **4** showed the V=O stretching vibrations at 985 and 867 cm^{-1}, respectively. Both **3** and **4** crystallize in space group $P2_12_12_1$ and their unit cell parameters are related. The molecular structures of **3** and **4** are shown in Figs. 10 and 11. Complex **3** has a five-coordinate square-pyramidal structure, while **4** has a polynuclear linear-chain structure. The V(1)–O(4′) distance is 2.290(6) Å, which is longer than the corresponding values for [VO{sal-(*R*,*R*)-stien}] · CH_3CN (**2**) (2.188(5) and 2.196(5) Å). A striking difference is observed between **3** and **4** in the conformation of the six-membered N–N chelate ring, and in the orientation of the ethoxy substituents. The six-membered N–N chelate ring of **3** has a distorted, flattened boat form with one methyl group (C(22)) in the axial position opposite to the oxo atom (O(4)) and the other methyl (C(19)) in the intermediate position between equatorial and axial positions (Fig. 10). On the other hand, in **4** the central N–N chelate ring has a chair form with one methyl group (C(19)) in the axial position on the same side of

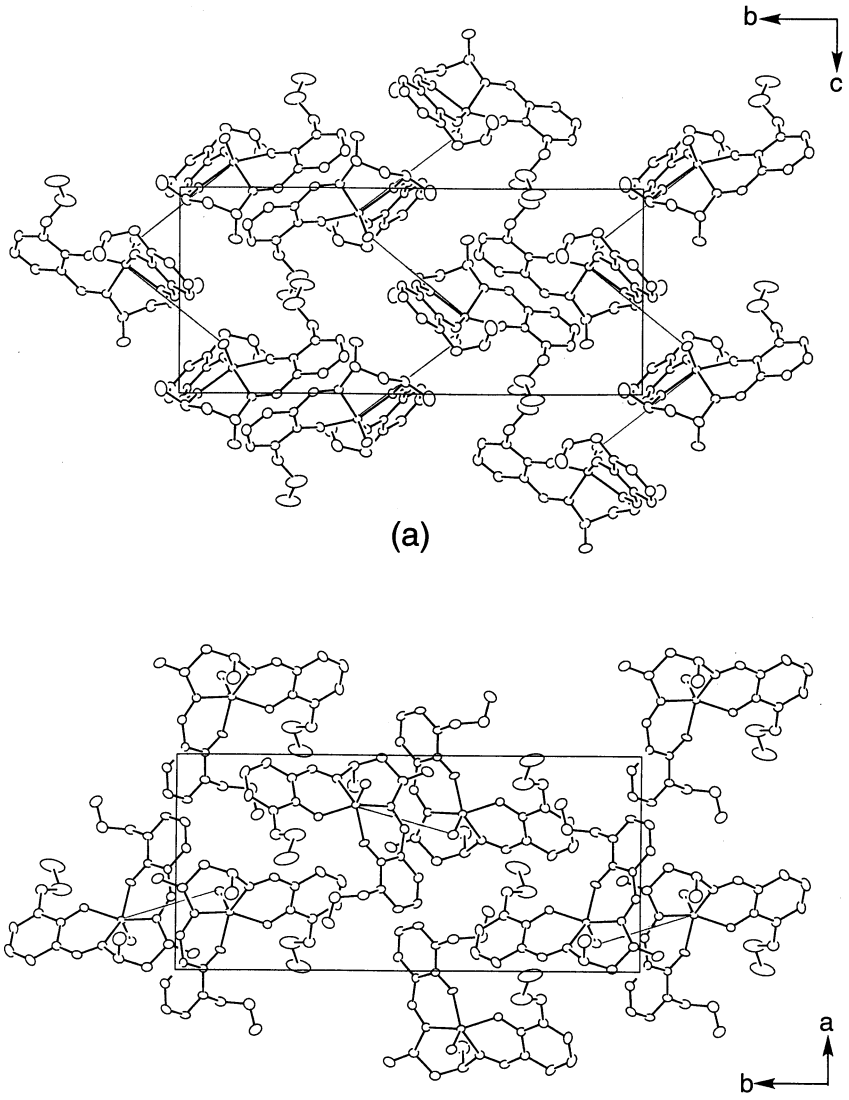

Fig. 12. Projections of the crystal structure of [VO{3-EtOsal-(*R*,*R*)-2,4-ptn}] (**3**) along the (a) *a*-axis, and (b) *c*-axis. Vanadium atoms and terminal oxygen atoms of the neighboring complexes are connected using solid lines to show the arrangement of the molecules. Reproduced with permission from Ref. [14].

the oxo atom (O(4)) and the other methyl group (C(22)) in the equatorial position (Fig. 11). The water molecule of **4** is hydrogen bonded to the four oxygen atoms of the ligand (O(2), O(3), O(5), and O(6)), the hydrogen bonded O···O distances being in the range 2.52(5)–3.45(3) Å. Both of the two ethoxy substituents of **4** are oriented in the equatorial position to form hydrogen bonds. There is no water of crystallization in **3**, and the ethoxy substituents are oriented opposite to each other in the axial positions. The steric effects of these axially-oriented methyl and ethoxy substituents seem to prevent any ···V=O···V=O··· linkage, and lead to the formation of a monomeric crystal structure for [VO{3-EtOsal-(*R*,*R*)-2,4-ptn}], even though Schiff base–oxovanadium(IV) complexes involving a six-membered N–N chelate ring usually have a linear chain structure.

Orange polymeric crystals of **4** were converted into green monomeric crystals of **3** upon heating at 170 °C for 10 min. Thermogravimetric measurements on **4** showed a loss of water of crystallization between 52 and 67 °C. An endothermic anomaly (6.0 ± 0.4 kJ mol^{-1}) assignable to the conversion from **4** to **3** was observed at 165 °C on a differential scanning calorimeter [14]. The X-ray studies and thermal analysis of **3** and **4** indicate that the structural changes occurring during the thermal conversion involve three processes: (i) a loss of water of crystallization and an orientational change of the ethoxy substituents; (ii) a rearrangement of the oxovanadium(IV) complexes from a polymeric to a monomeric structure; and (iii) a conformational change of the six-membered N–N chelate ring from a chair to a flattened boat form. Figs. 12 and 13 show the

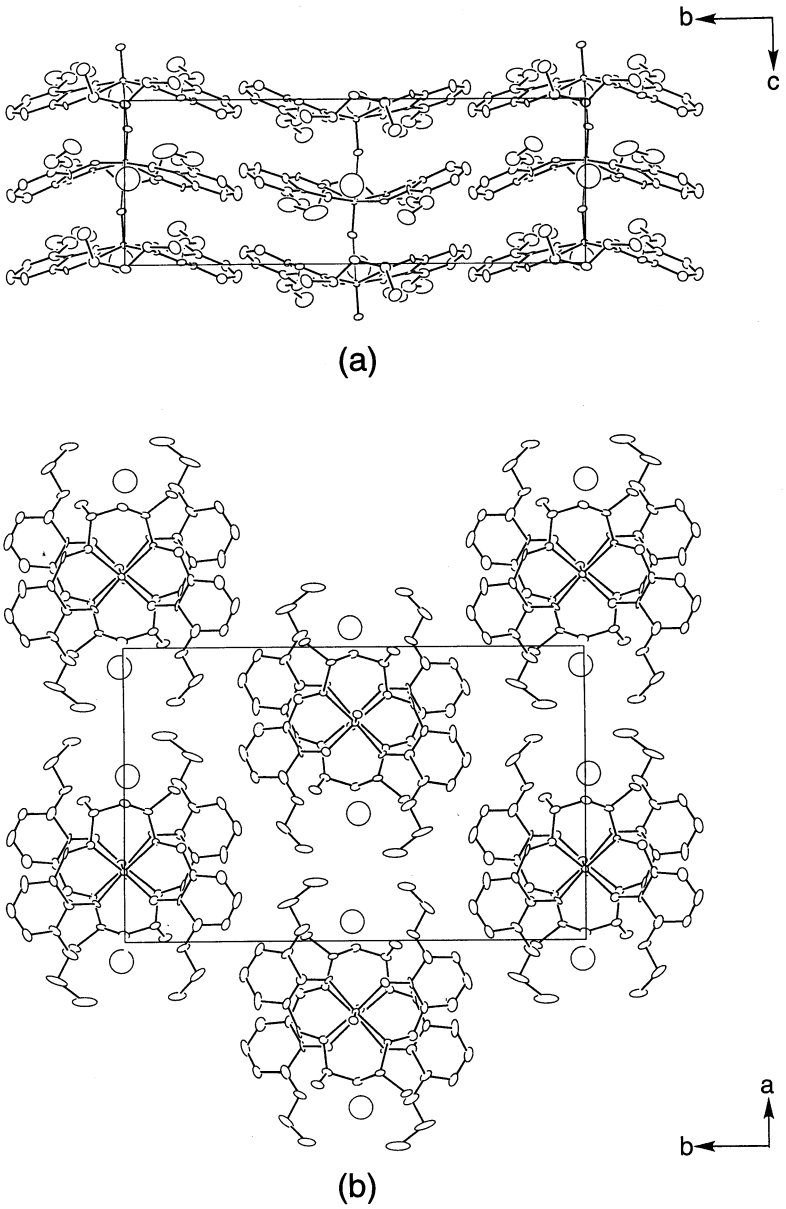

Fig. 13. Projections of the crystal structure of [VO{3-EtOsal-(*R*,*R*)-2,4-ptn}] · H_2O (**4**) along the *a*-axis, and (b) *c*-axis. Vanadium atoms and terminal oxygen atoms of the neighboring complexes are connected using solid lines to show the arrangement of the molecules. Reproduced with permission from Ref. [14].

packing diagrams of **3** and **4** viewed along the *a* and *c* axes. In **4**, the linear ···V=O···V=O··· chains run along the 2_1 screw axes parallel to the *c* axis. The six-membered N–N chelate rings in polymeric chains are arranged in an alternate up-and-down pattern along the *a* direction. After the loss of water of crystallization, the complexes alternately slide with some rotation along the $\pm b$ direction, and the ···V=O···V=O··· linkage is broken on heating to yield the monomeric **3**. The conformation of the six-membered N–N chelate ring is converted from the chair to the boat form during the structural transformation.

Oxovanadium(IV) complexes, [VO{Xsal-(*R*,*R*)-2,4-ptn}] (X = 3-MeO, 5-MeO, 5-Br, and 5-NO_2; Fig. 1) having electron donating or electron withdrawing groups at the three- or five-position of the salicylaldehyde moieties have been prepared, and the electronic influence of the substituents on the formation of monomeric and polymeric structures was investigated [15]. The 5-MeO complex, with electron donating groups, forms a monomeric structure. The other [VO{Xsal-(*R*,*R*)-2,4-ptn}] (X = H, 3-MeO, 5-Br, 5-NO_2) complexes exhibited only polymeric structures. The structures and the redox potentials for the V(V)/

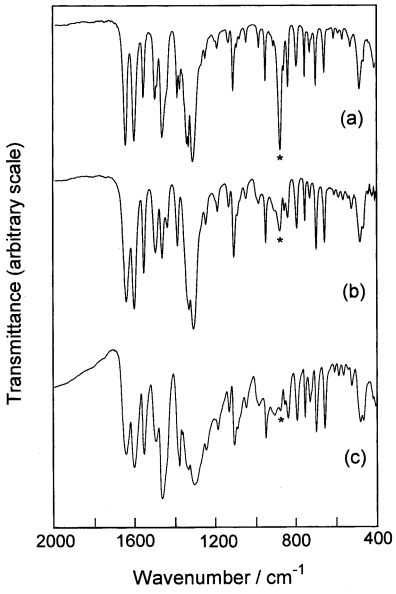

Fig. 14. The IR spectra of (a) $[VO(5\text{-}NO_2salen)] \cdot 2H_2O$ (**5**) in a Nujol mull, (b) (**5**) in a KBr pellet, and (c) the ground product of **5** in a Nujol mull.

V(IV) couple of the complexes in dimethyl sulfoxide have been compared. The results indicate that a complex with a lower potential tends to form a monomeric structure rather than a polymeric one.

2.3. Mechanochemical reaction of polymeric $[VO(5\text{-}NO_2salen)] \cdot 2H_2O$

The light brown $[VO(5\text{-}NO_2salen)] \cdot 2H_2O$ complex (**5**) ($H_2$5-NO_2salen = *N*,*N*′-di-5-nitrosalicylidene-1,2-ethanediamine) has a linear chain structure in the solid state. Complex **5** shows a strong V=O stretching IR band at 875 cm^{-1} in a Nujol mull (Fig. 14) in accord with the polymeric structure. The intensity of the band decreased when the spectrum was measured in a KBr disk [16]. The complex turned dark brown on grinding thoroughly in a mortar. The IR spectrum of this dark brown product was similar to that of **5** in a Nujol mull, however, the intensity of the V=O stretching band decreased significantly and all bands broadened (Fig. 14). This mechanochemical behavior is different from the mechanochemical conversion from a polymeric to a monomeric form as observed for $[VO\{sal\text{-}(R,R)\text{-}stien\}] \cdot CH_3CN$ (**2**). When **2** was ground in a mortar, the color changed from orange to green, and the intensity of the V=O stretching band of the polymeric form (860 cm^{-1}) decreased with a complementary increase of the V=O stretching band attributable to the monomeric form (990 cm^{-1}). On the other hand, only a decrease in intensity of the V=O stretching band at 875 cm^{-1} was observed and no band assignable to the V=O stretching of the monomeric species was detected in the spectrum of the ground product of **5**. The ground product is amorphous as evidenced by the X-ray powder diffraction pattern. The temperature dependence of the magnetic susceptibilities revealed that the ferromagnetic interactions between the molecules in the chains of **5** decreased on grinding. The spectroscopic and magnetic data suggest that grinding of **5** cleaves the ···V=O···V=O··· bonds to yield various fragments of the polymeric chains. These fragments will be inhomogeneous in their size and shapes, and have different V=O stretching frequencies. As there are so many species with different V=O stretching frequencies, the V=O stretching bands of the ground product will be too weak to be observed.

3. Isomerization of a Schiff base–oxovanadium(IV) complex

3.1. Isomerization between a pair of diastereomers of $[VO\{3\text{-}EtOsal,sal\text{-}(R,R)\text{-}chxn\}]$

Thermal isomerization between a pair of diastereomers of the oxovanadium(IV) complex with an unsymmetrical tetradentate Schiff base ligand, **I** and **II** of [VO{3-EtOsal,sal-(*R*,*R*)-chxn}] (Fig. 15), has been studied at 195 °C [9]. The two isomers, **I** and **II**, were separated using silica gel column chromatography. The green forms, **I** (green) and **II** (green), were isolated by crystallization from dichloromethane. The orange forms, **I** (orange) and **II** (orange), were obtained by suspending the green crystals of the respective isomers in an acetonitrile–water mixture (1:2 v/v) under nitrogen. The green and orange forms were assigned as the monomeric and polymeric species, respectively, on the basis of the V=O stretching frequencies. All four

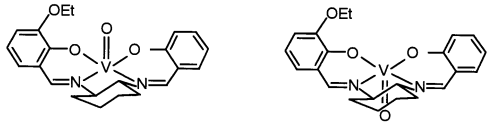

Fig. 15. The two isomers of [VO{3-EtOsal,sal-(*R*,*R*)-chxn}].

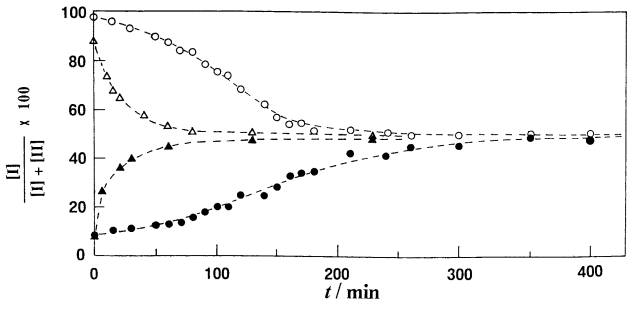

Fig. 16. A reaction profile of [VO{3-EtOsal,sal-(*R*,*R*)-chxn}] at 195 °C: △, **I** (orange); ▲, **II** (orange); ○, **I** (green); ●, **II** (green). Reproduced with permission from Ref. [9].

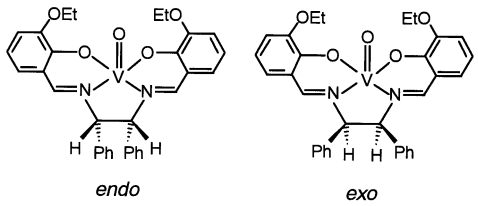

Fig. 17. The *endo*- and *exo*-isomers of [VO(3-EtOsal-*meso*-stien)].

complexes possess water of crystallization. Thermogravimetric analysis on the four compounds showed that water of crystallization was easily lost below 110 °C.

The four complexes, **I** (green), **II** (green), **I** (orange), and **II** (orange), were heated at 195 °C in the solid state. The progress of the isomerization between isomers **I** and **II** was followed by a high-performance liquid chromatographic method. Fig. 16 shows the percentage of isomer **I** versus reaction time. No isomerization took place during the process of the isomer distribution analysis. There was no difference between the results of reactions carried out in air or in a nitrogen atmosphere. The orange complexes, **I** (orange) and **II** (orange), isomerized much faster than the green complexes, and after 1 h, the reactions attained equilibrium, **I**:**II** ≈ 1:1. The orange complexes have a linear chain structure, and the isomerization may have taken place by migration of the terminal oxygen (V=O) to an adjacent vanadium. However, the reactions were accompanied by a color change; the orange complexes turned green within a few minutes at 195 °C, indicating a disassembling of the chain structure. It should be noted that the isomerization proceeded after the complexes disassembled to monomeric five-coordinate green complexes, where there would have been no vanadium in the neighborhood of the terminal oxygen atom. The green complexes, **I** (green) and **II** (green), isomerized much more slowly than the orange complexes, and no color change was observed. These results may suggest that the green complexes formed by heating the orange complexes have a different crystal structure from those of the original green complexes, **I** (green) and **II** (green).

3.2. Isomerization from the endo-[VO(3-EtOsal-meso-stien)] isomer to the exo-isomer

The *endo*- and *exo*-isomers of [VO(3-EtOsal-*meso*-stien)] ($H_2$3-EtOsal-*meso*-stien = *N*,*N*′-di-3-ethoxysalicylidene-(*R*,*S*)(*S*,*R*)-1,2-diphenyl-1,2-ethanediamine, Figs. 1 and 17) were prepared separately. The *endo*-isomer isomerized to the *exo*-isomer upon heating at

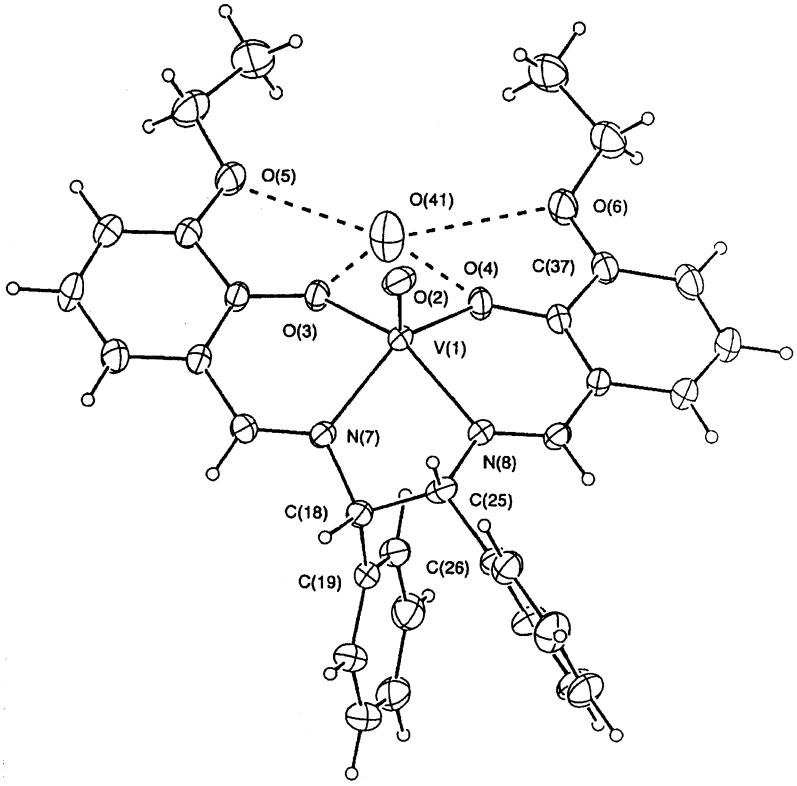

Fig. 18. An ORTEP drawing of *endo*-[VO(3-EtOsal-*meso*-stien)] · $3H_2O$. O(41) is the oxygen atom of a water of crystallization, and hydrogen bonds are indicated with broken lines. Reproduced with permission from Ref. [17].

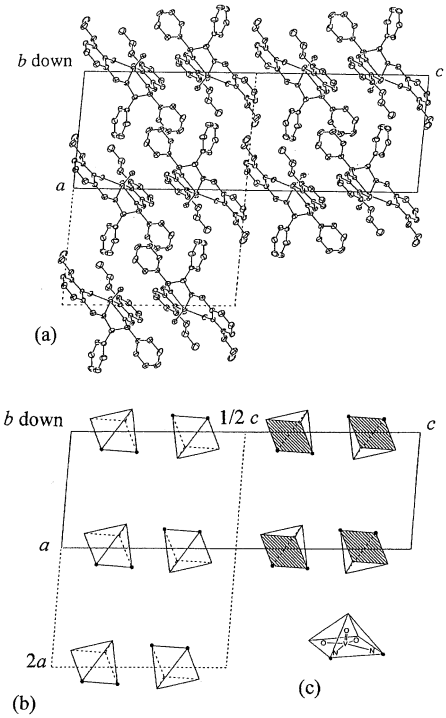

Fig. 19. (a) Projection of the crystal structure of *endo*-[VO(3-EtOsal-*meso*-stien)] · $3H_2O$ as viewed down the *b*-axis. Water molecules of crystallization are omitted for clarity. (b) Schematic drawing of the arrangement of the complexes with square-pyramidal coordination. The basal planes of square-pyramids are hatched if they are directed upward. (c) Definition of the square-pyramid, where two corners corresponding to the N atoms are indicated by closed circles. Reproduced with permission from Ref. [17].

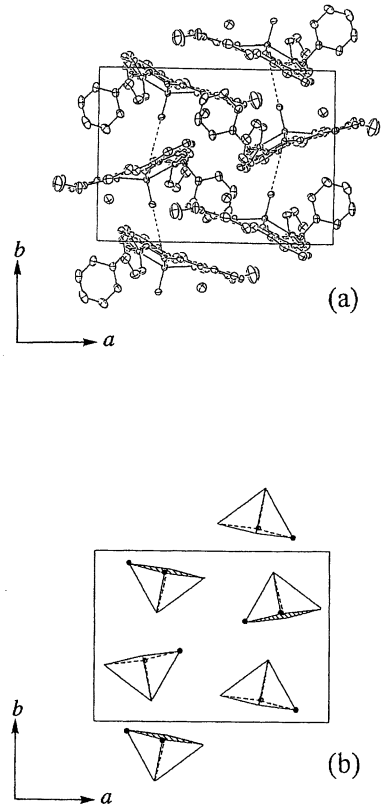

Fig. 20. (a) Projection of the crystal structure of *exo*-[VO(3-EtOsal-*meso*-stien)] · H_2O as viewed up the *c*-axis. (b) Schematic drawing of the arrangement of the complexes with square-pyramidal coordination. Reproduced with permission from Ref. [17].

210 °C for 20 h in an argon atmosphere [17]. When the reaction was carried out in the air, the thermal dehydrogenation of the ligand occurred at benzylic carbon atom sites to form a C=C double bond (vide infra). The *endo*-[VO(3-EtOsal-*meso*-stien)] · $3H_2O$ crystallized in space group $P2_1/c$, and the molecular structure is shown in Fig. 18. The crystal structure is shown in Fig. 19 with a schematic drawing, where the positions and orientations of the VN_2O_3 square-pyramid are indicated. The structure of the thermal product was assigned as the *exo*-isomer on the basis of the X-ray powder-diffraction profile. The crystal structure of the *exo*-isomer is shown in Fig. 20 for comparison. The space group is $P2_1/n$, and the V=O bonds lie nearly on the 2_1 screw axis parallel to *b* to form a weak linear-chain structure. The crystal transformation from the *endo*-isomer to the *exo*-isomer accompanies a drastic rearrangement of the individual complex molecules. Although the solvent molecules of crystallization are lost below 100 °C, and there may be some void space in the crystals, such a drastic molecular rearrangement will not be topochemical [18].

4. Thermal dehydrogenation

During the course of our investigation into the thermal reactions of oxovanadium(IV) complexes, the green monomeric *exo*-[VO(3-EtOsal-*meso*-stien)] complex was heated at 190 °C for 8 h in the air in the solid state to obtain an orange product, [VO(3-EtOsalton)] (**6**) in a 45% yield [8]. We expected the transformation from a monomeric to a polymeric structure on the basis of the color. However, the IR spectrum of **6** showed the V=O stretching band at 973 cm^{-1}, which is indicative of a monomeric structure. Moreover, the color of an acetonitrile solution was orange. A polynuclear orange complex disassembles in solution to give a green solution (vide supra). Thus, the orange complex **6** does not seem to have a linear chain structure. The structure was determined by X-ray diffraction, and the result provided definitive evidence that the complex is monomeric, and that dehydrogenation took place at the two benzylic carbon atoms to form a C=C double bond (Figs. 21 and 22). The geometry around the vanadium atom is a distorted octahedron, with a weak coordination of one water molecule (V(1)–O(81) distance: 2.406(3) Å) *trans* to the oxo ligand. The V(1) atom is displaced 0.339(3) Å from the equatorial N_2O_2 coordi-

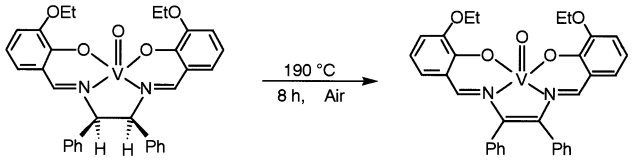

Fig. 21. The thermal dehydrogenation of [VO(3-EtOsal-*meso*-stien)] to form [VO(3-EtOsalton)] (**6**) in the solid state.

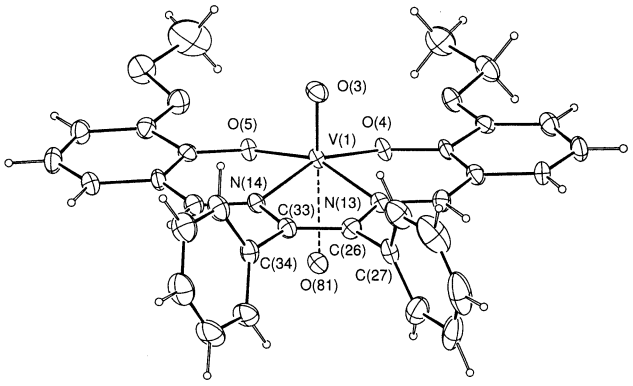

Fig. 22. An ORTEP drawing of [VO(3-EtOsalton)] (**6**). Reproduced with permission from Ref. [8].

nation plane. The five-membered N–N chelate ring is almost flat, with two phenyl groups in the equatorial positions. The C(26)–C(33) bond distance (1.353(6) Å), and the bond angles around C(26) and C(33) (116.6(4)–123.3(4)°), indicate a C=C double bond in the five-membered chelate ring moiety.

The dehydrogenation reaction was accompanied by the formation of a dark brown vanadium(V) byproduct. The reaction under an oxygen atmosphere was about twice as fast as that in air, and the reaction did not occur in an argon atmosphere. No thermal dehydrogenation was observed for the free H_2X-sal-*meso*-stien ligands. When a ligand was heated at 190 °C in air, only the decomposition reaction took place. The rate of the thermal dehydrogenation reaction of [VO(Xsal-*meso*-stien)] was influenced by the substituents (X). The introduction of electron-donating groups at the three- or five-position of the salicylaldehyde moieties (X = 3-EtO, 5-MeO) accelerated the reaction. Dehydrogenation of the complex did not occur with electron-withdrawing 5-NO_2 substituents. The transformation of [VO{3-EtOsal-(*R*,*R*)-stien}] into **6** also occurred. However, the yield was lower (22%) than that for [VO(3-EtOsal-*meso*-stien)] under the same conditions (190 °C for 8 h). This fact indicates that the *cis* configuration of the two hydrogen atoms of the five-membered N–N chelate ring in [VO(3-EtOsal-*meso*-stien)] is preferable for the dehydrogenation reaction to the *trans* configuration of the hydrogen atoms in [VO{3-EtOsal-(*R*,*R*)-stien}].

In order to elucidate the reaction mechanism, we studied the dehydrogenation reactions of nickel(II) complexes [19]. Red [Ni(3-EtOsalton)] (**7**) (Figs. 1 and 23) was easily prepared from [Ni(3-EtOsal-*meso*-stien)] in dioxane with DDQ (2,3-dichloro-5,5-dicyano-1,4-benzoquinone) as an oxidant. In the solid, the thermal dehydrogenation of [Ni(3-EtOsal-*meso*-stien)] did not occur on heating in air at 210 °C for 15 h. On the other hand, on heating a mixture of [Ni(3-EtOsal-*meso*-stien)] and [VO(salen)] powders in air at 190 °C for 17 h, **7** was obtained in a 24% yield. Heating [Ni(3-EtOsal-*meso*-stien)] with [VO(salen)]NO_3 at 160 °C for 50 h under argon also yielded **7** in a 54% yield (Fig. 24). These facts indicate that the nickel complex is dehydrogenated by $[V^{V}O(salen)]^{+}$, which is formed from [VO(salen)] with atmospheric oxygen on heating. On the basis of these results, the oxidants of the thermal dehydrogenation reactions of oxovanadium(IV) complexes are suggested to be the vanadium(V) species originating from the oxovanadium(IV) complexes. The formation of the V^{V} species was observed as a byproduct (see above).

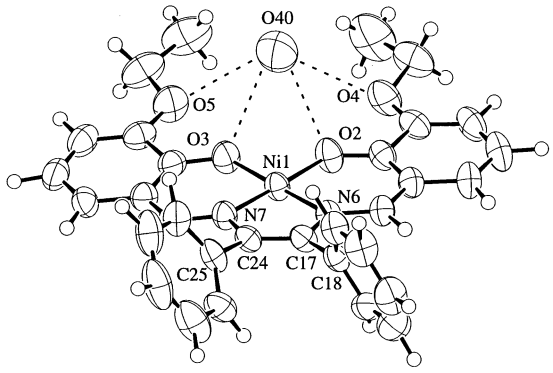

Fig. 23. An ORTEP drawing of [Ni(3-EtOsalton)] · CH_3OH · 1.33H_2O (**7**). O40 is the oxygen atom of a water of crystallization, and the hydrogen bonds are indicated by broken lines. Reproduced with permission from Ref. [19].

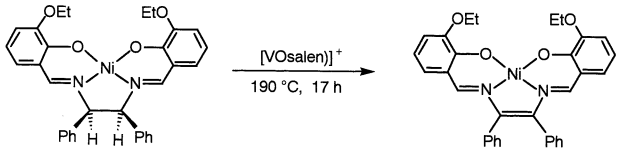

Fig. 24. The thermal dehydrogenation of [Ni(3-EtOsal-*meso*-stien)] by $[VO(salen)]^{+}$ in the solid state.

Acknowledgements

This work was supported by the Iketani Science and Technology Foundation and by a grant-in-aid for scientific research on priority area (no. 1136236) from the Ministry of Education, Culture, Sports, Science and Technology, Japan.

References

[1] K. Nakajima, M. Kojima, J. Fujita, Chem. Lett. (1986) 1483.
[2] K. Nakajima, K. Kojima, M. Kojima, Bull. Chem. Soc. Jpn. 63 (1990) 2620.
[3] M. Mathew, A.J. Carty, G.J. Palenik, J. Am. Chem. Soc. 92 (1970) 3197.
[4] A. Serrette, P.J. Carroll, T.M. Swager, J. Am. Chem. Soc. 114 (1992) 1887.
[5] S.A. Fairhurst, D.L. Hughes, U. Kleinkes, G.J. Leigh, J.R. Sanders, J. Weisner, J. Chem. Soc. Dalton Trans. (1995) 321.
[6] M. Kojima, K. Nakajima, M. Tsuchimoto, P.M. Treichel, S. Kashino, Y. Yoshikawa, Proc. Jpn. Acad. Ser. B 71 (1995) 175.
[7] K. Nakajima, M. Kojima, S. Azuma, R. Kasahara, M. Tsuchimoto, Y. Kubozono, H. Maeda, S. Kashino, S. Ohba, Y. Yoshikawa, J. Fujita, Bull. Chem. Soc. Jpn. 69 (1996) 3207.
[8] G. Hoshina, M. Tsuchimoto, S. Ohba, K. Nakajima, H. Uekusa, Y. Ohashi, H. Ishida, M. Kojima, Inorg. Chem. 37 (1998) 142.
[9] M. Kojima, K. Nakajima, M. Tsuchimoto, M. Tanaka, T. Suzuta, Y. Yoshikawa, J. Fujita, Chem. Lett. (1994) 949.
[10] A. Pasini, M. Gullotti, J. Coord. Chem. 3 (1974) 319.
[11] E. Cariati, J. Bourassa, P.C. Ford, Chem. Commun. (1998) 1623.
[12] E. Cariati, X. Bu, P.C. Ford, Chem. Mater. 12 (2000) 3385.
[13] C.A. Root, J.D. Hoeschele, C.R. Cornman, J.W. Kampf, V.L. Pecoraro, Inorg. Chem. 32 (1993) 3855.
[14] R. Kasahara, M. Tsuchimoto, S. Ohba, K. Nakajima, H. Ishida, M. Kojima, Inorg. Chem. 26 (1996) 7661.
[15] M. Tsuchimoto, R. Kasahara, K. Nakajima, M. Kojima, Polyhedron 18 (1999) 3035.
[16] M. Tsuchimoto, G. Hoshina, N. Yoshioka, H. Inoue, K. Nakajima, M. Kamishima, M. Kojima, S. Ohba, J. Solid State Chem. 153 (2000) 9.
[17] G. Hoshina, S. Ohba, K. Nakajima, H. Ishida, M. Kojima, M. Tsuchimoto, Bull. Chem. Soc. Jpn. 72 (1999) 1037.
[18] M.D. Cohen, Z. Ludmer, J.M. Thomas, J.O. Williams, Proc. R. Soc. Lond. Ser. A 324 (1971) 459.
[19] G. Hoshina, M. Tsuchimoto, S. Ohba, Bull. Chem. Soc. Jpn. 73 (2000) 369.